

Deterministic CNOT Gate on electron qubits using quantum-dot spins in double-sided optical microcavities

Hai-Rui Wei and Fu-Guo Deng*

*Department of Physics, Applied Optics Beijing Area Major Laboratory,
Beijing Normal University, Beijing 100875, China*

(Dated: January 27, 2023)

We propose a scheme to construct a deterministic CNOT gate on static electron-spin qubits, allowing for deterministic scalable quantum computing in solid-state systems. The excess electron confined in a charged quantum dot inside a double-sided optical microcavity represents the qubit, and the single photons play a medium role. Moreover, our device can work in both the weak coupling and the strong coupling regimes, but high fidelities are achieved only when the ratio of the side leakage to the cavity loss is low. Finally, we assess the feasibility of this device and show it can be implemented with current technology.

PACS numbers: 03.67.Lx, 78.67.Hc, 42.50.Pq, 03.67.Mn

The controlled-not (CNOT) gate has numerous applications in the field of quantum information science and it is one of the elementary elements for a quantum computer [1–3]. In 1995, Barenco *et al.* [4] proven that any n -qubit quantum computation can be achieved by using a sequence of one-qubit gates and CNOT gates. The archetypal two-qubit CNOT gate, or its equivalents, have been demonstrated from various perspectives and for different physical systems, including trapped ions [5, 6], nuclear magnetic spins [7], superconducting circuits [8, 9], and linear optics [10, 11]. In fact, each of these systems has its bottleneck. For example, based on linear optical elements, the maximum probability for achieving a CNOT gate is $3/4$ [12]. A Superconducting circuit is fragile to decoherence. In 2004, Beenakker *et al.* [13] proposed a theoretic protocol for CNOT gate on moving electrons. Nemoto and Munro [14] introduced a protocol for a CNOT gate on photons with cross-Kerr nonlinearity. The CNOT gate on static qubits is more useful for a scalable quantum computing.

Recent works show that the electron spin in a quantum dot (QD) [15] can be used to store and process quantum information due to the long electron-spin coherence time ($\sim \mu\text{s}$) [16] using spin echo techniques, which is limited by the spin relaxation time ($\sim \text{ms}$) [17], and it hold great promising in quantum communications, quantum information processing, and quantum networks. The spin-QD-cavity unit, e.g., an electron confined in a self-assembled In(Ga)As QD or a GaAs interface QD inside a single-sided or a double-sided optical resonant cavity was proposed by Hu *et al.* [18, 19]. In this unit, the spin represents the qubit and promises scalable quantum information computing. A single spin qubit can be read out by the information of a coupling photon, and spin manipulation is well developed using pulsed magnetic-resonance technique. This unit has been used for constructing a hybrid CNOT gate and a phase-shift

gate, two-photon Bell-state analyzer (BSA), teleportation, entanglement swapping, entanglement purification, and creating photon-photon, photon-spin, and spin-spin entanglements [18–24].

In this paper, we investigate the construction of a CNOT gate on the two static electrons confined in two charged QDs inside two double-sided microcavities. We first propose a device which can convert the spin parity into the out-coming photon polarization information. Using two such parity measurements, we construct a CNOT gate on two static electron-spin qubits, resorting to an ancilla static electron-spin qubit, a single-qubit measurement, and the application of single-qubit operations. Moreover, a complete deterministic two-spin BSA was constructed. In our scheme, the CNOT gate promises a scalable quantum computing in solid-state systems, in which two single photons only are mediums. The device works in both the weak coupling and the strong coupling regimes, but high fidelities are achieved only when the side leakage and cavity loss is low.

The spin-QD-double-side-cavity unit, we consider here, is a singly electron charged self-assembled GaAs/InAs interface QD inside an optical resonant double-sided microcavity with two partially reflective mirrors. The potential of this system has also been recognized in Ref.[19]. An exciton (X^-) that consists of two electrons and a hole can be created by optical excitation. Here, the dipole is resonant with cavity mode, probed with a resonant light. The four relevant electronic levels are shown in Fig.1. [19]. Due to Pauli's exclusion principle, there are two dipole transitions, one involving a photon with the spin $s_z = +1$ and the other involving a photon with $s_z = -1$. Considering a photon with $s_z = \pm 1$, if the injecting photon coupled to the dipole, the cavity is reflected, and both the polarization and the propagation direction of the photon will be flipped. Otherwise, the cavity is transmissive and the photon will acquire a $\pi \bmod 2\pi$ phase shift relative to a reflected photon. The rules of the input states changed under the interaction of the photons with $s_z = \pm 1$ and the cavity are described

*Corresponding author: fgdeng@bnu.edu.cn

as follows:

$$\begin{aligned}
 |R^\uparrow \uparrow\rangle &\rightarrow |L^\downarrow \uparrow\rangle, & |L^\uparrow \uparrow\rangle &\rightarrow -|L^\uparrow \uparrow\rangle, \\
 |R^\downarrow \uparrow\rangle &\rightarrow -|R^\downarrow \uparrow\rangle, & |L^\downarrow \uparrow\rangle &\rightarrow |R^\uparrow \uparrow\rangle, \\
 |R^\uparrow \downarrow\rangle &\rightarrow -|R^\uparrow \downarrow\rangle, & |L^\uparrow \downarrow\rangle &\rightarrow |R^\downarrow \downarrow\rangle, \\
 |R^\downarrow \downarrow\rangle &\rightarrow |L^\uparrow \downarrow\rangle, & |L^\downarrow \downarrow\rangle &\rightarrow -|L^\downarrow \downarrow\rangle.
 \end{aligned} \quad (1)$$

Here, $|\uparrow\rangle$ and $|\downarrow\rangle$ represent the electron-spin states $|+\frac{1}{2}\rangle$ and $|-\frac{1}{2}\rangle$, respectively. The spin quantization axis for angular momentum is along the normal direction of cavity that is the z axis. $|R\rangle$ ($|L\rangle$) is the right (left) circular polarization of a photon, and the superscripts \uparrow and \downarrow indicate the propagation directions of a photon along the z axis. In Fig.1, $|\uparrow\rangle$ and $|\downarrow\rangle$ represent hole-spin states $|+\frac{3}{2}\rangle$ and $|-\frac{3}{2}\rangle$, respectively.

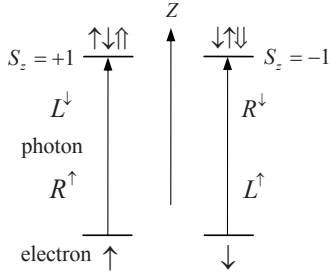


FIG. 1: Relevant energy levels and spin selection rules for optical transition of negatively charged exciton X^- .

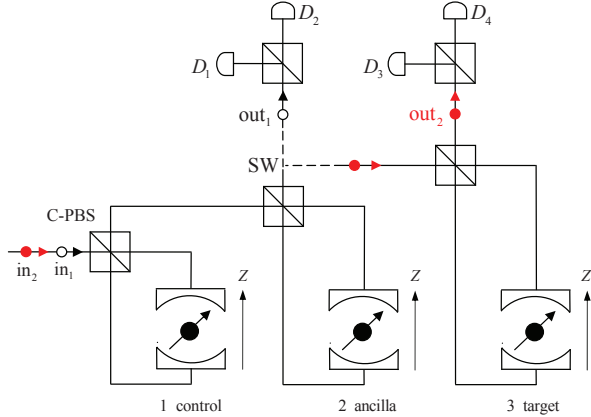


FIG. 2: (Color online) Scheme for a CNOT gate on noninteracting static electron-spin qubits inside the double-sided microcavities. D_i ($i = 1, 2, 3, 4$) are four single-photon detectors. The polarizing beam splitter in the circular basis (C-PBS) transmits a right-circular polarization photon $|R\rangle$ and reflects a left-circular polarization photon $|L\rangle$. SW is an optical switch. After the first PCG on the control qubit and the ancilla qubit, the first C-PBS is rotated by 90° , so that the second probe photon $|L\rangle$ (label in_2) deserts the first cavity and injects directly into the cavities 2 and 3 in sequence.

Now, let us describe the procedure for the construction of the parity-check gate (PCG) and a CNOT gate for spin-QD-double-side-cavity units. Based on the rules discussed above, the principle of our PCG for two spin qubits (in the first two cavities) is shown in Fig.2. It is relied on the spin-to-polarization conversion. Two excess electron spins in the cavities are in two arbitrary states. A probe photon passes through the polarizing beam splitter in the circuit basis (C-PBS) and it injects into the first and the second cavities in succession. After it interacts with the cavities, the photon is detected. By detecting the output of the photon, one can distinguish the spin states of the two-electron system $\{|\uparrow_1\uparrow_2\rangle, |\downarrow_1\downarrow_2\rangle\}$ from $\{|\uparrow_1\downarrow_2\rangle, |\downarrow_1\uparrow_2\rangle\}$. If the two spins are parallel ($|\uparrow_1\uparrow_2\rangle$ or $|\downarrow_1\downarrow_2\rangle$), the polarization of the probe photon in the state $|R\rangle$ ($|L\rangle$) will remain and the photon will trigger the detector D_2 (D_1); otherwise, the state of the probe photon will be flipped and the photon will be detected by the detector D_1 (D_2). The evolution of the photon-cavity state can be described as

$$\begin{aligned}
 |R^\downarrow\rangle|\uparrow_1\uparrow_2\rangle &\rightarrow |R^\downarrow\rangle|\uparrow_1\uparrow_2\rangle, & |R^\downarrow\rangle|\uparrow_1\downarrow_2\rangle &\rightarrow -|L^\uparrow\rangle|\uparrow_1\downarrow_2\rangle, \\
 |R^\downarrow\rangle|\downarrow_1\downarrow_2\rangle &\rightarrow |R^\downarrow\rangle|\downarrow_1\downarrow_2\rangle, & |R^\downarrow\rangle|\downarrow_1\uparrow_2\rangle &\rightarrow -|L^\uparrow\rangle|\downarrow_1\uparrow_2\rangle, \\
 |L^\uparrow\rangle|\uparrow_1\uparrow_2\rangle &\rightarrow |L^\uparrow\rangle|\uparrow_1\uparrow_2\rangle, & |L^\uparrow\rangle|\uparrow_1\downarrow_2\rangle &\rightarrow -|R^\downarrow\rangle|\uparrow_1\downarrow_2\rangle, \\
 |L^\uparrow\rangle|\downarrow_1\downarrow_2\rangle &\rightarrow |L^\uparrow\rangle|\downarrow_1\downarrow_2\rangle, & |L^\uparrow\rangle|\downarrow_1\uparrow_2\rangle &\rightarrow -|R^\downarrow\rangle|\downarrow_1\uparrow_2\rangle.
 \end{aligned} \quad (2)$$

Based on spin-QD-double-side-cavity systems, the principle of our CNOT gate is shown in Fig.2. It is used to flips the spin of the target qubit if the spin of the control qubit is $|\downarrow\rangle$; otherwise, it does nothing. Suppose that the two excess electron spins in the first cavity and third cavity are considered as the control qubit and the target qubit, respectively. They are in two arbitrary states $|\psi_1^s\rangle = \alpha_1|\uparrow_1\rangle + \beta_1|\downarrow_1\rangle$ and $|\psi_3^s\rangle = \alpha_3|\uparrow_3\rangle + \beta_3|\downarrow_3\rangle$, respectively. The ancilla qubit in the second cavity is prepared in the state $|\psi_{anci}^s\rangle = \frac{1}{\sqrt{2}}(|\uparrow_2\rangle + |\downarrow_2\rangle)$. Our scheme consists of three parts. (i) We take two PCGs on spin pairs 1-2 and 2-3 in series, with a Hadamard transformation (e.g., using a $\pi/2$ microwave pulse)

$$|\uparrow\rangle \rightarrow \frac{1}{\sqrt{2}}(|\uparrow\rangle + |\downarrow\rangle), \quad |\downarrow\rangle \rightarrow \frac{1}{\sqrt{2}}(|\uparrow\rangle - |\downarrow\rangle), \quad (3)$$

on the ancilla qubit and target qubit before and after the second PCG operation, respectively. The first probe photon (label in_1) is originally in state $|R_1^\uparrow\rangle$ and the second one (label in_2) is in $|L_2^\uparrow\rangle$. (ii) The ancilla qubit is measured. (iii) According to the result of two PCGs and the spin of the ancilla qubit, a proper classical feed-forward is performed on the control qubit and the target qubit to complete a CNOT gate with the success probability of 100%. The correspondences between the results of each measurements and specific feed-forwards are given in Table I.

BSA is an important prerequisite for many quantum protocols, such as superdense coding, teleportation, entanglement swapping, and so on. Next, based on spin-QD-double-side-cavity units, we show the principle of our

TABLE I: The correspondences between the results of two PCG operations and the spin of the ancilla and the feed-forward operators applied to the control and the target spins in the construction of a static two-spin-qubit CNOT gate.

PCG1	PCG2	ancilla qubit	feedforward	
			control qubit	target qubit
R	L	\uparrow		
		\downarrow		σ_x
	R	\uparrow	$-\sigma_z$	
		\downarrow	σ_z	σ_x
L	L	\uparrow		σ_x
		\downarrow		
	R	\uparrow	$-\sigma_z$	σ_x
		\downarrow	σ_z	

complete BSA for Fermionic two-qubit systems. It can be implemented with the left two parts shown in Fig.2. Considering the system composed of the two excess electrons in cavities 1 and 2. It is prepared in the four Bell states

$$\begin{aligned} |\psi^\pm\rangle &= \frac{1}{\sqrt{2}}(|\uparrow_1\uparrow_2\rangle \pm |\downarrow_1\downarrow_2\rangle), \\ |\varphi^\pm\rangle &= \frac{1}{\sqrt{2}}(|\uparrow_1\downarrow_2\rangle \pm |\downarrow_1\uparrow_2\rangle). \end{aligned} \quad (4)$$

After the PCG operation is performed on the qubits 1 and 2 (the inject probe photon, labeled as in_1 , is in state $|R_1\rangle$), the four Bell states are divided into two groups. That is, $|\psi^\pm\rangle$ and $|\varphi^\pm\rangle$. $|\psi^\pm\rangle$ correspond to the click of the detector D_2 , and $|\varphi^\pm\rangle$ correspond to D_1 . The "+" state and the "-" state in each group can be distinguished by the same operation of PCG on the system in the second time after a Hadamard operation is performed on both the control and the target qubits. In detail, the "+" state corresponds to the click of the detector D_2 , and the "-" state corresponds to D_1 . This scheme can be extended to create remote multi-spin entangled states such as Greenberger-Horne-Zeilinger states (GHZ) or cluster states [26].

By far, we have shown the principles for PCG, CNOT gates, and BSA under the ideal condition. We consider imperfections due to side leakage of cavity field, the trion dephasing, and the heavy-light hole mixing. To calculate the fidelity of the CNOT gate, we have to use the reflection and transmission operators of a singly charged QD inside an optical double-sided microcavity to describe the photon-spin entangling gate, i.e.,

$$\begin{aligned} \hat{t}(\omega) &= t_0(\omega)(|R\rangle\langle R| \otimes |\uparrow\rangle\langle\uparrow| + |L\rangle\langle L| \otimes |\downarrow\rangle\langle\downarrow|) + \\ &\quad t(\omega)(|R\rangle\langle R| \otimes |\downarrow\rangle\langle\downarrow| + |L\rangle\langle L| \otimes |\uparrow\rangle\langle\uparrow|), \\ \hat{r}(\omega) &= r_0(\omega)(|R\rangle\langle R| \otimes |\uparrow\rangle\langle\uparrow| + |L\rangle\langle L| \otimes |\downarrow\rangle\langle\downarrow|) + \\ &\quad r(\omega)(|R\rangle\langle R| \otimes |\downarrow\rangle\langle\downarrow| + |L\rangle\langle L| \otimes |\uparrow\rangle\langle\uparrow|). \end{aligned} \quad (5)$$

Here, $r_0(\omega)$, $t_0(\omega)$, and $r(\omega)$, $t(\omega)$ are the reflection and the transmission coefficients of the uncoupled and the

coupled cavities, respectively. Both operators include the contributions from the uncoupled and the coupled cavities. From [19], r and t in the system can be described as

$$\begin{aligned} r(\omega) &= 1 + t(\omega), \\ t(\omega) &= \frac{-\kappa[i(\omega_{X^-} - \omega) + \frac{\gamma}{2}]}{[i(\omega_{X^-} - \omega) + \frac{\gamma}{2}][i(\omega_c - \omega) + \kappa + \frac{\kappa_s}{2}] + g^2} \end{aligned} \quad (6)$$

where ω , ω_c , and ω_{X^-} are the frequencies of the input photon, cavity mode, and X^- transition, respectively. g is cavity coupling strength and $\gamma/2$ is the X^- dipole decay rate. κ and $\kappa_s/2$ are the cavity field decay rates into the input/output modes and the leaky modes, respectively.

In our schemes, we consider the resonance with $\omega_c = \omega_{X^-} = \omega$. By taking $g = 0$, we get the reflection and the transmission coefficients $r_0(\omega)$ and $t_0(\omega)$ for an empty cavity (or call it a cold cavity) where the QD does not couple to the cavity, and

$$t_0(\omega) = -\frac{\kappa}{\kappa + \frac{\kappa_s}{2}}, \quad r_0(\omega) = \frac{\frac{\kappa_s}{2}}{\kappa + \frac{\kappa_s}{2}}. \quad (7)$$

Otherwise,

$$r(\omega) = 1 + t(\omega), \quad t(\omega) = -\frac{\frac{\gamma}{2}\kappa}{\frac{\gamma}{2}[\kappa + \frac{\kappa_s}{2}] + g^2}, \quad (8)$$

for a hot cavity ($g \neq 0$).

If the side leakage and cavity loss rate κ_s is much lower than the output coupling rate κ (the ideal case), we have $|t_0(\omega)| \rightarrow 1$, $|r_0(\omega)| \rightarrow 0$ for the cold cavity and $|t(\omega)| \rightarrow 0$, $|r(\omega)| \rightarrow 1$ for the hot cavity in the strong coupling regime $g > (\kappa, \gamma)$. Thus the transmission and the reflection operators can be simplified as

$$\begin{aligned} \hat{t}(\omega) &= t_0(\omega)(|R\rangle\langle R| \otimes |\uparrow\rangle\langle\uparrow| + |L\rangle\langle L| \otimes |\downarrow\rangle\langle\downarrow|), \\ \hat{r}(\omega) &= r(\omega)(|R\rangle\langle R| \otimes |\downarrow\rangle\langle\downarrow| + |L\rangle\langle L| \otimes |\uparrow\rangle\langle\uparrow|). \end{aligned} \quad (9)$$

That is, our scheme for a CNOT gate can achieve a unity fidelity in the strong-coupling regime. However, this is a big challenge for QD-micropillar cavities although significant progress has been made [27]. If the cavity side leakage κ_s which will cause bit-flip error is taken into account, we have

$$\begin{aligned} |R^\downarrow\downarrow\rangle &\rightarrow |r||L^\uparrow\downarrow\rangle + |t||R^\downarrow\downarrow\rangle, \\ |L^\uparrow\downarrow\rangle &\rightarrow |r||R^\downarrow\downarrow\rangle + |t||L^\uparrow\downarrow\rangle, \\ |R^\downarrow\uparrow\rangle &\rightarrow -|t_0||R^\downarrow\uparrow\rangle - |r_0||L^\uparrow\uparrow\rangle, \\ |L^\uparrow\uparrow\rangle &\rightarrow -|t_0||L^\uparrow\uparrow\rangle - |r_0||R^\downarrow\uparrow\rangle. \end{aligned} \quad (10)$$

The fidelity of the CNOT gate can be written as

$$\begin{aligned} F &= 1 - P, \\ &= \frac{(\frac{\kappa_s}{\kappa})^4 + 16}{(\frac{\kappa_s}{\kappa})^4 + 16(\frac{\kappa_s}{\kappa})^2 + 16} = \frac{200(\frac{g}{\kappa})^4 + 1}{200(\frac{g}{\kappa})^4 + 3}, \end{aligned} \quad (11)$$

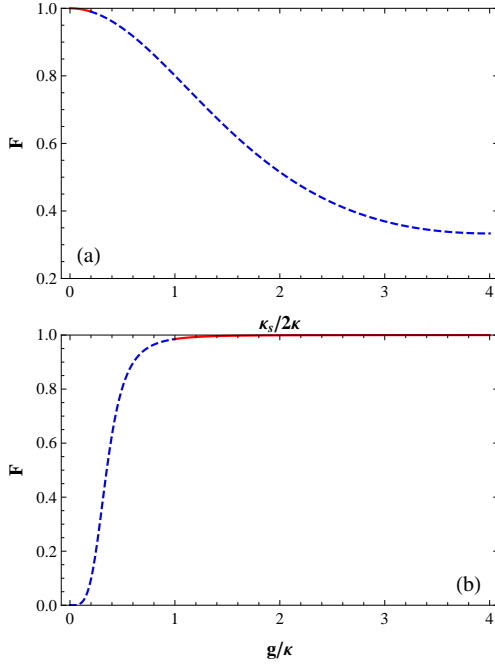


FIG. 3: (Color online) (a) The fidelity of the CNOT gate vs the side leakage rate κ_s . (b) The fidelity of the CNOT gate vs the coupling strength. $\gamma = 0.1\kappa$ which is experimentally achievable and $|r| = |t_0|$ (that is, $\frac{g^2}{\kappa^2} = \frac{\kappa}{10\kappa_s} - \frac{\kappa_s}{40\kappa}$) which is required for our protocol are taken for (a)-(b), and $\omega_c = \omega_{X^-} = \omega = \omega_0$ is assumed.

by taking $\gamma = 0.1\kappa$ which is experimentally achieved, $|t_0| = |r|$ (that is, $(\frac{g}{\kappa})^2 = \frac{\kappa}{10\kappa_s} - \frac{\kappa_s}{40\kappa}$) which is required for our protocol, and $\omega_c = \omega_{X^-} = \omega$. Here P is the error rate.

As shown in Fig.3(a) and Fig.3(b), a near-unity fidelity of the CNOT gate can be achieved with small $\kappa_s/2\kappa$ in the strong-coupling regime with $g/\kappa = 2.4$, which can be achieved for the In(Ga)As QD-cavity system [27, 28]. The lower $\kappa_s/2\kappa$, the higher F . A higher fidelity could also be achieved by taking a lower $\kappa_s/2\kappa$ in the weak-coupling regime $g < (\gamma, \kappa)$.

The exciton dephasing reduces the fidelity by a amount of $[1 - \exp(-\tau/T_2)]$, where τ is the cavity photon lifetime and T_2 is the trion coherence time. Two kinds of dephasing processes should be considered here: the optical dephasing and the spin dephasing of X^- . For optical dephasing, it can reduce slightly the fidelity by only a few percents as the optical coherence time of excitons in self-assembled In(Ga)As QDs can be as long as several hundred picoseconds [29], ten times long as the cavity photon lifetime (around tens of picoseconds in the strong coupling regime for a cavity with a Q-factor of $10^4 - 10^5$). For spin dephasing of the X^- which mainly arises from the hole-spin dephasing, it can be safely neglected in our considerations, because spin coherence time is at least three order of the magnitude longer than the cavity photon lifetime [30, 31].

For a realistic QD, the imperfect optical selection rule, due to the heavy-light hole mixing, can also reduce the fidelity by a few percents as the hole mixing in the valence band is in the order of a few percents [32] [e.g., for self-assembled In(Ga)As QDs]. The hole mixing could be reduced by engineering the shape and the size of QDs or choosing different types of QDs.

In summary, we have proposed a device which can convert the spin parity of two static electron-spin qubits confined in charged QDs inside double-sided microcavities into the out-coming photon polarization information. Using two such parity-check measurements, we construct a deterministic CNOT gate on electron-spin qubits, allowing for deterministic scalable quantum computing in solid-state systems. Subsequently, a possible application of the spin-QD-double-side-cavity, a spin Bell-state analyzer was discussed. Moreover, from the investigation on the fidelity of the CNOT gate, one can find that our proposal works in both the weak coupling and the strong coupling regimes, but high fidelities are achieved only when the ratio of the side leakage to the cavity loss is low.

This work is supported by the National Natural Science Foundation of China under Grant Nos. 10974020 and 11174039, NCET-11-0031, and the Fundamental Research Funds for the Central Universities.

-
- [1] M. A. Nielsen and I. L. Chuang, *Quantum Computation and Quantum Information* (Cambridge University Press, Cambridge, 2000).
 - [2] C. Monroe *et al.*, Phys. Rev. Lett. **75**, 4714 (1995).
 - [3] A. Barenco, D. Deutsch, A. Ekert, and R. Jozsa, Phys. Rev. Lett. **74**, 4083 (1995).
 - [4] A. Barenco *et al.*, Phys. Rev. A **52**, 3457 (1995).
 - [5] C. Monroe *et al.*, Phys. Rev. Lett. **75**, 4714 (1995).
 - [6] F. Schmidt-Kaler *et al.*, Nature (London) **422**, 408 (2003).
 - [7] A. M. Childs, I. L. Chuang, and D. W. Leung, Phys. Rev. A **64**, 012314 (2001).
 - [8] T. Yamamoto *et al.*, Nature (London) **425**, 941 (2003).
 - [9] J. H. Plantenberg *et al.*, Nature (London) **447**, 836 (2007).
 - [10] J. L. O'Brien *et al.*, Nature (London) **426**, 264 (2003).
 - [11] T. B. Pittman, M. J. Fitch, B. C. Jacobs, and J. D. Franston, Phys. Rev. A **68**, 032316 (2003).
 - [12] E. Knill, R. Laflamme, and G. J. Milburn, Nature (London) **409**, 46 (2001).
 - [13] C. W. J. Beenakker, D. P. DiVincenzo, C. Emary, and M. Kindermann, Phys. Rev. Lett. **93**, 020501 (2004).
 - [14] K. Nemoto, and W. J. Munro, Phys. Rev. Lett. **93**, 250502 (2004).
 - [15] D. Loss and D. P. DiVincenzo, Phys. Rev. A **57**, 120 (1998); A. Imamoglu *et al.*, Phys. Rev. Lett. **83**, 4204

- (1999); C. Piermarocchi, P. C. Chen, L. J. Sham, and D. G. Steel, *ibid.* **89**, 167402 (2002); T. Calarco *et al.*, Phys. Rev. A **68**, 012310 (2003); S. M. Clark, Kai-Mei C. Fu, T. D. Ladd, and Y. Yamamoto, Phys. Rev. Lett. **99**, 040501 (2007); Z. R. Lin *et al.*, *ibid.* **101**, 230501 (2008).
- [16] J. R. Petta *et al.*, Science **309**, 2180 (2005); A. Greilich *et al.*, *ibid.* **313**, 341 (2006).
- [17] J. M. Elzerman *et al.*, Nature (London) **430**, 431 (2004); M. Kroutvar *et al.*, *ibid.* **432**, 81 (2004).
- [18] C. Y. Hu *et al.*, Phys. Rev. B **78**, 085307 (2008).
- [19] C. Y. Hu, W. J. Munro, J. L. O'Brien, and J. G. Rarity, Phys. Rev. B **80**, 205326 (2009).
- [20] C. Y. Hu, W. J. Munro, and J. G. Rarity, Phys. Rev. B **78**, 125318 (2008).
- [21] C. Y. Hu, and J. G. Rarity, Phys. Rev. B **83**, 115303 (2011).
- [22] C. Bonato *et al.*, Phys. Rev. Lett. **104**, 160503 (2010).
- [23] C. Wang, Y. Zhang, and G. S. Jin, Phys. Rev. A **84**, 032307 (2011).
- [24] T. Yu *et al.*, Phys. Scr. **84**, 025001 (2011).
- [25] R. J. Warburton *et al.*, Phys. Rev. Lett. **79**, 5282 (1997).
- [26] X. L. Zhang, M. Feng, and K. L. Gao, Phys. Rev. A **73**, 014301 (2006).
- [27] S. Reitzenstein *et al.*, Appl. Phys. Lett. **90**, 251109 (2007).
- [28] J. P. Reithmaier *et al.*, Nature (London) **432**, 197 (2004); T. Yoshie *et al.*, *ibid.* **432**, 200 (2004); E. Peter *et al.*, Phys. Rev. Lett. **95**, 067401 (2005).
- [29] P. Borri *et al.*, Phys. Rev. Lett. **87**, 157401 (2001); D. Birkedal, K. Leosson, and J. M. Hvam, *ibid.* **87**, 227401 (2001); W. Langbein *et al.*, Phys. Rev. B **70**, 033301 (2004).
- [30] D. Heiss *et al.*, Phys. Rev. B **76**, 241306 (2007); B. D. Gerardot *et al.*, Nature (London) **451**, 441 (2008).
- [31] D. Brunner *et al.*, Science **325**, 70 (2009).
- [32] G. Bester, S. Nair, and A. Zunger, Phys. Rev. B **67**, 161306 (2003).